Supporting information

One-step Synthesis of Modified Ti_3C_2 MXene Supported Amorphous Molybdenum Sulfide Electrocatalysts by Facile Gamma Radiation Strategy for Efficient Hydrogen Evolution Reaction

Shuangxiao Li,[1] *Xueyan Que,*[1] *Xibang Chen,*[1,2] *Tingrui Lin*,[1,3] *Lang Sheng*,[1] *Jing Peng*,[1,*] *Jiuqiang Li,*[1] *and Maolin Zhai* [1,*]

[1] Beijing National Laboratory for Molecular Sciences, Radiochemistry and Radiation Chemistry Key Laboratory of Fundamental Science, the Key Laboratory of Polymer Chemistry and Physics of the Ministry of Education, College of Chemistry and Molecular Engineering, Peking University, Beijing 100871, China.

[2] Institute of Chemical Defense, Beijing 100191, China

[3] Skshu Paint Co., Ltd., Putian 351100, P. R. China

*Corresponding authors

*E-mail: mlzhai@pku.edu.cn Tel: +86-010-62753794.

*E-mail: jpeng@pku.edu.cn Tel: +86-010-62757193.

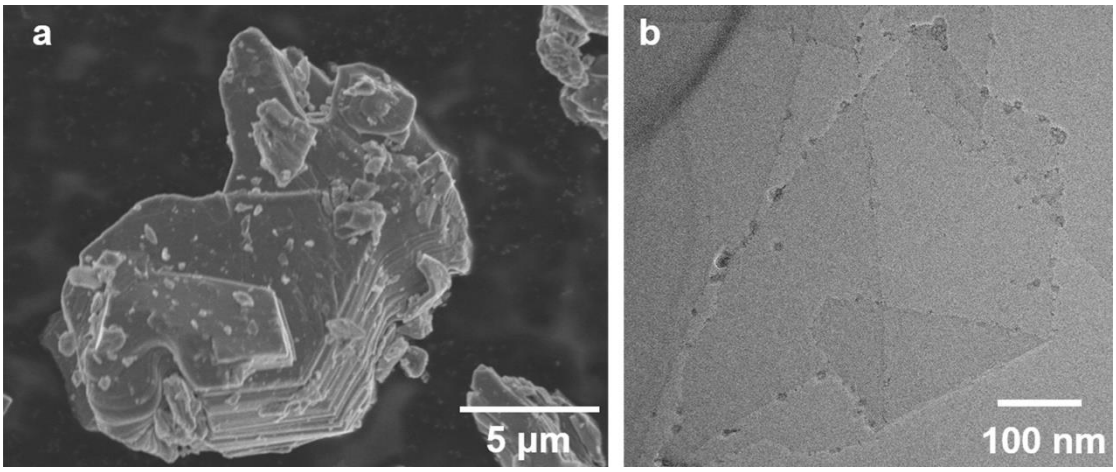

Figure S1. Morphological characterization of (a)Ti_3AlC_2 (SEM image) (b) pristine Ti_3C_2 nanosheets (TEM image)

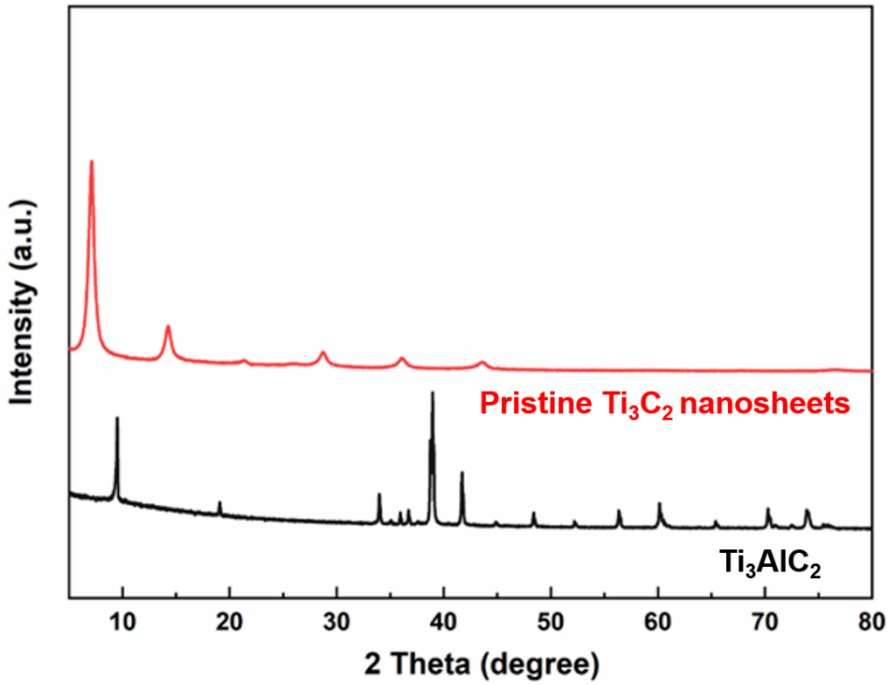

Figure S2. XRD patterns of pristine Ti_3C_2 MXene nanosheets and Ti_3AlC_2

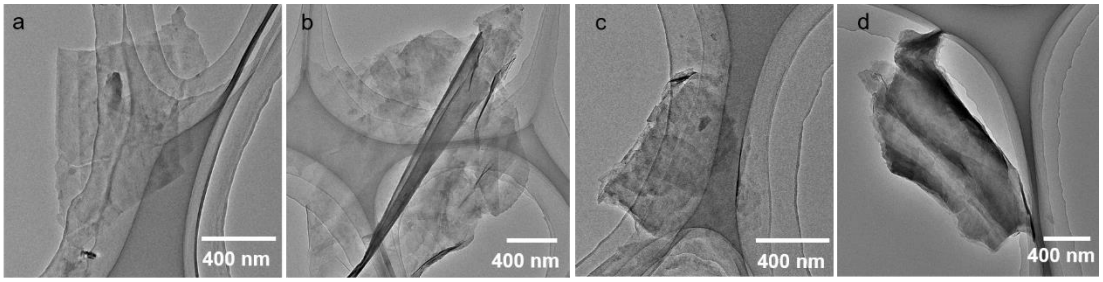

Figure S3. TEM images of MD-Ti_3C_2/MoS_x hybrids synthesized at different absorbed doses. (a). MD-Ti_3C_2/MoS_x-50 (b). MD-Ti_3C_2/MoS_x-100 (c). MD-Ti_3C_2/MoS_x-200 (d) MD-Ti_3C_2/MoS_x-300

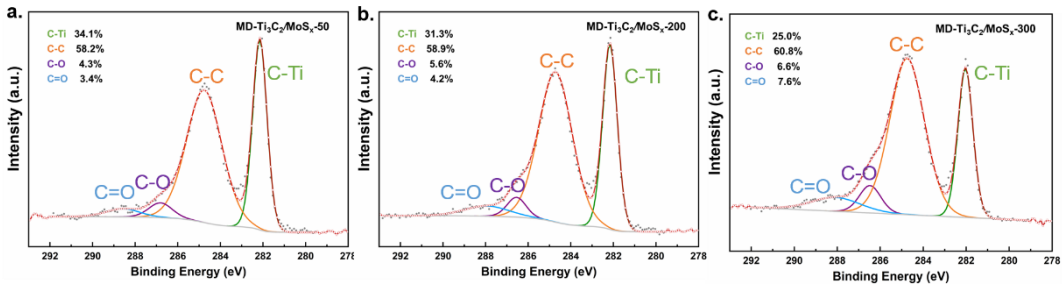

Figure S4. High resolution XPS of C 1s spectra of (a) MD-Ti_3C_2/MoS_x-50 (b) MD-Ti_3C_2/MoS_x-200 and (c) MD-Ti_3C_2/MoS_x-300

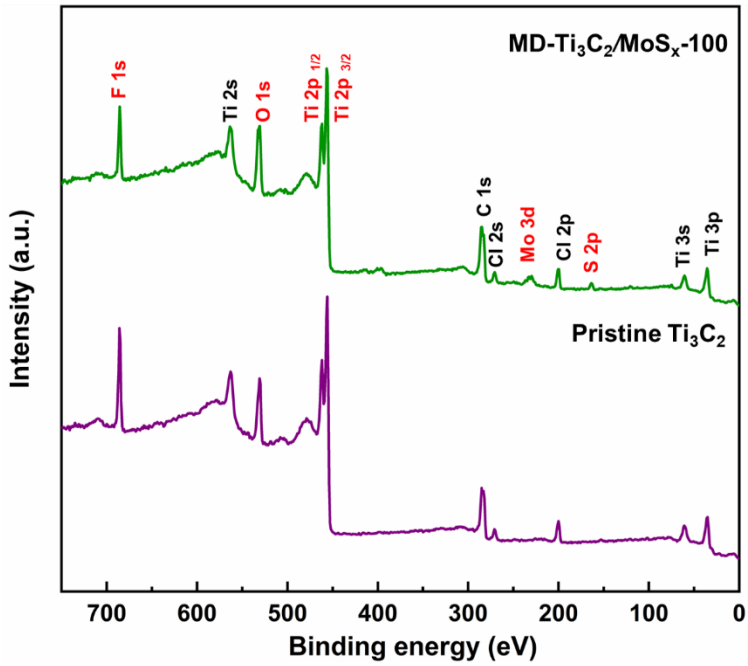

Figure S5. XPS survey spectra of MD-Ti_3C_2/MoS_x-100 and pristine Ti_3C_2.

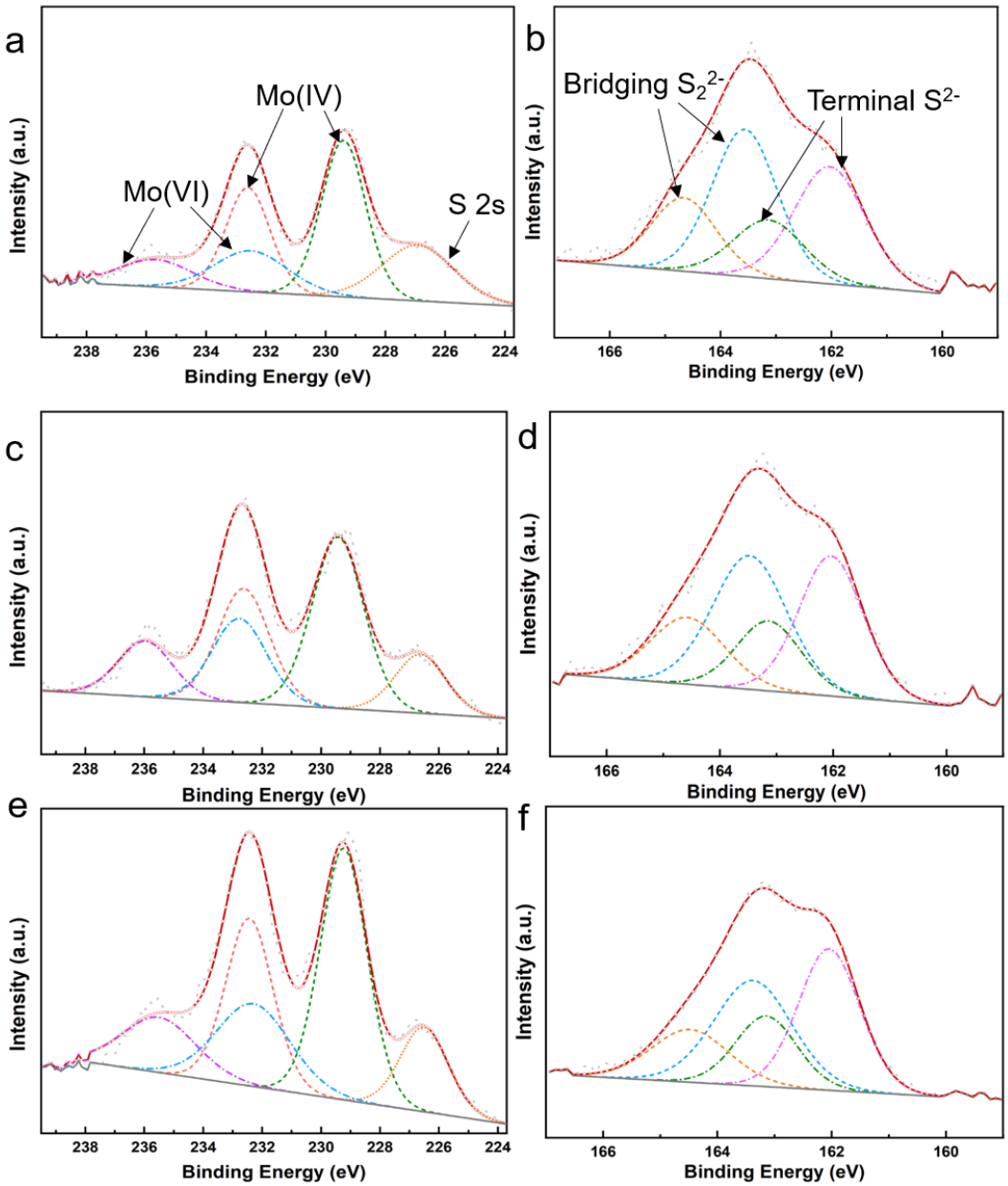

Figure S6. High resolution XPS of Mo 3d and S 2p spectra of (a)(b) MD-Ti_3C_2/MoS_x-50, (c)(d) MD-Ti_3C_2/MoS_x-200 and (e)(f) MD-Ti_3C_2/MoS_x-300, respectively.

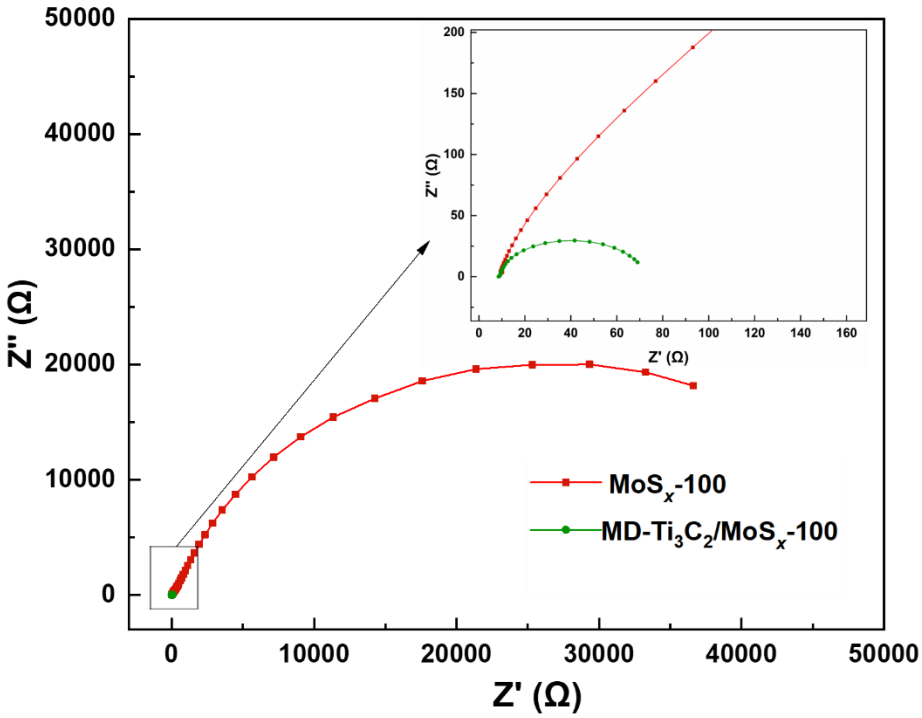

Figure S7. Electrochemical impedance spectroscopy of MoS_x-100 and MD-Ti_3C_2/MoS_x-100, inset is the enlarged results of the selective region.

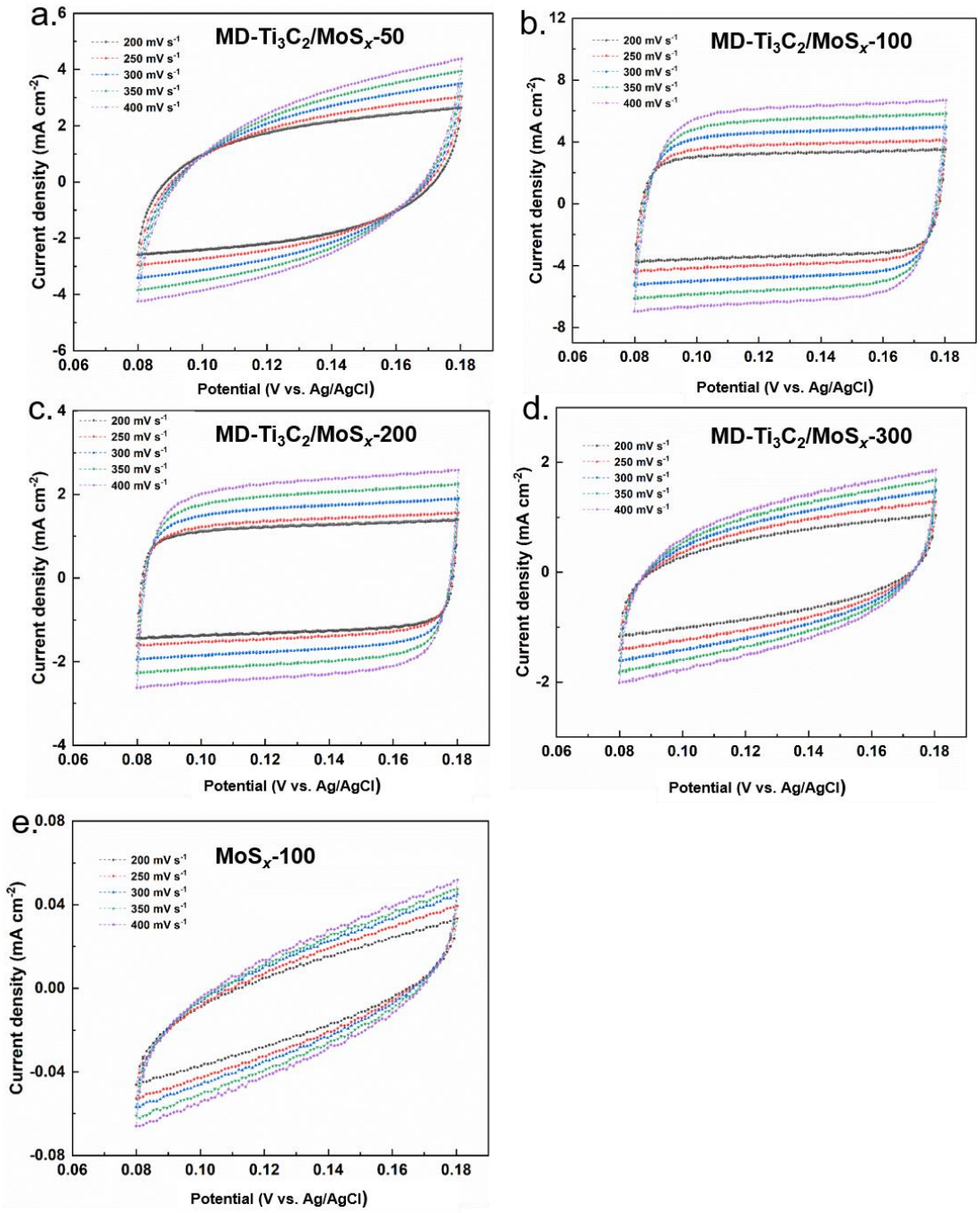

Figure S8. Cyclic voltammetry curves obtained in 0.5 M H_2SO_4 from 80 to 180 mV *vs* Ag/AgCl of (a) MD-Ti_3C_2/MoS_x-50, (b) MD-Ti_3C_2/MoS_x-100, (c) MD-Ti_3C_2/MoS_x-200, (d) MD-Ti_3C_2/MoS_x-300 and (e) MoS_x-100. The legend on the top left corner gives the scan rates.

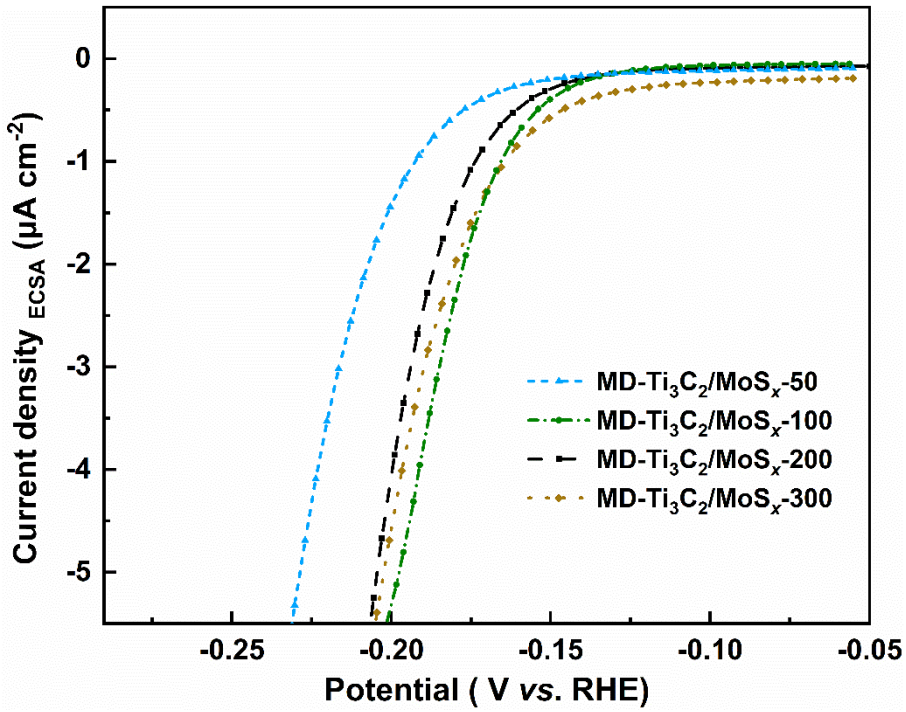

Figure S9. Polarization curves (normalized by ECSA) of MD-Ti_3C_2/MoS_x-50, MD-Ti_3C_2/MoS_x-100, MD-Ti_3C_2/MoS_x-200 and MD-Ti_3C_2/MoS_x-300. The ECSA was derived from the C_{dl} (40 μF cm^{-2} was used for specific capacitance value).

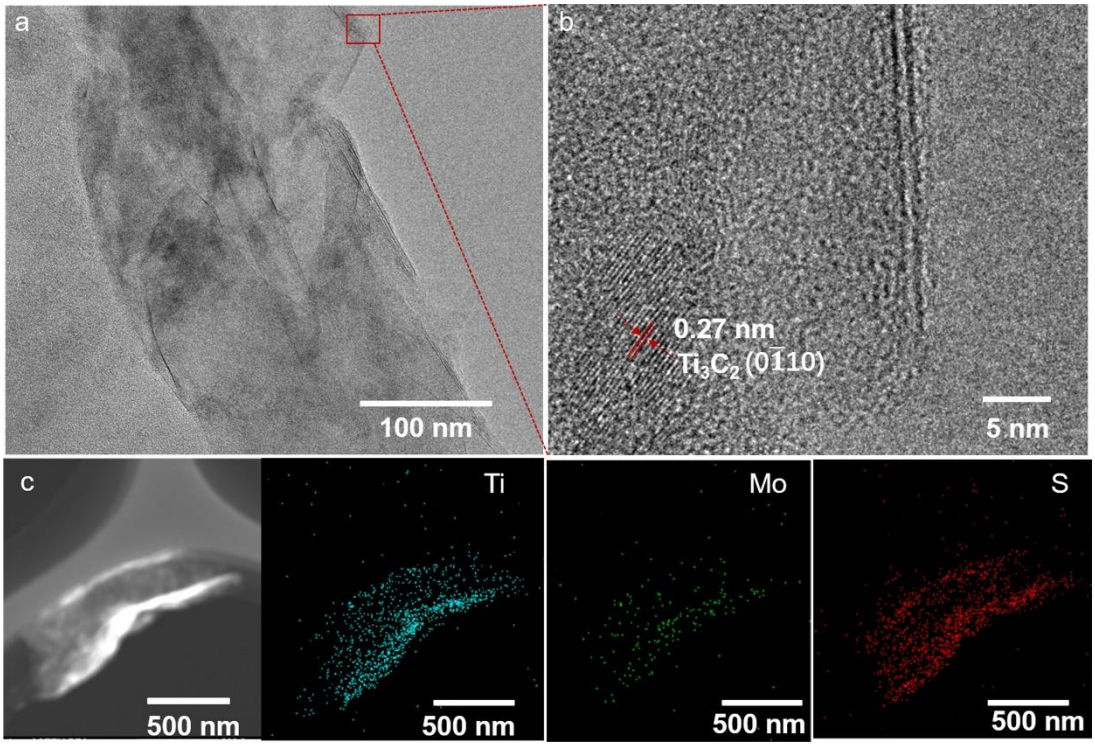

Figure S10. TEM images of (a) MD-Ti_3C_2/MoS_x-100 after HER and (b) the enlarged image of the selected region in (a); (c) EDS mappings of Ti (blue), Mo (green) and S (red) of the selected region in MD-Ti_3C_2/MoS_x-100 after HER.

Table S1. The standard potentials of radicals produced in the gamma radiation process and the proposed reaction.

Radicals	Standard potential (V *vs* SHE)	Reference
e_{aq}^-	-2.87	[1]
OH·	1.90	[2]
H·	-2.30	[1]
$HO_2^{\cdot}$	0.79	[3]
$(CH_3)_2COH\cdot$	-1.80	[1]

The proposed reaction for MoS_x generation is shown in reaction (1) and reaction (2)

$$MoS_4^{2-} + e_{aq}^- \longrightarrow MoS_x + S^{2-} \quad (1)$$

$$MoS_4^{2-} + (CH_3)_2\dot{C}OH \longrightarrow MoS_x + S^{2-} + (CH_3)_2CO + H^+ \quad (2)$$

Table S2. Atomic ratio of Mo, S, Ti of MoS_x-100 and MD-Ti_3C_2/MoS_x hybrids synthesized at different absorbed doses from XPS results.

samples	MoS_x -100	MD-Ti_3C_2/MoS_x -50	MD-Ti_3C_2/MoS_x -100	MD-Ti_3C_2/MoS_x -200	MD-Ti_3C_2/MoS_x -300
Mo/Ti (%)	-	5.0	9.7	9.8	19.0
S/Mo	1.9	2.5	2.2	2.0	1.8

Table S3. XPS results of S content, ratio and the content of S atoms with higher binding energy of MD-Ti_3C_2/MoS_x hybrids synthesized at different absorbed doses.

samples	S-high/S-low	S content (at%)	S-high content (at%)
MD-Ti_3C_2/MoS_x-50	1.12	2.53	1.33
MD-Ti_3C_2/MoS_x-100	1.09	3.53	1.84
MD-Ti_3C_2/MoS_x-200	1.06	2.87	1.47
MD-Ti_3C_2/MoS_x-300	0.90	5.75	2.72

S-high: bridging S_2^{2-} with higher binding energy

S-low: terminal S^{2-} with lower binding energy

Table S4. Comparison of MD-Ti_3C_2/MoS_x-100 in this work with the related works reported in recent three years (in 0.5M H_2SO_4).

Samples	Synthetic method	η_{10} (mV)	Tafel slope (mV dec^{-1})	Reference
Vertically aligned $MoS_2 \perp Ti_3C_2T_x$	Microwave synthetic method	110	40	[4]
"nanoroll" like $MoS_2/Ti_3C_2T_x$	Nitrogen-freezing and annealing	152	70	[5]
Hierarchical $MoS_2/Ti_3C_2T_x$	Hydrothermal	280	68	[6]
Amorphous MoS_x fim on Ti substrate	electrodeposition	211	55	[7]
Amorphous MoS_x/TNAs	electrodeposition	157	53	[8]
Amorphous MoS_x/CNTs	Ultrasonic spray	168	36	[9]
$MoS_2@Mo_2CT_x$	hydrothermal	176	114	[10]
MD-Ti_3C_2/MoS_x-100	γ-ray radiation	165	41	This work

References

1. Belloni, J.; Mostafavi, M.; Remita, H.; Marignier, J.-L.; Marie-Odile Delcourt, a.. *New Journal of Chemistry*, **1998**, 22, 1239-1255.
2. C. Dispenza, N. Grimaldi, M. A. Sabatino, I. L. Soroka and M. Jonsson, *Journal of Nanoscience and Nanotechnology*, **2015**, 15, 3445-3467.
3. Koppenol, W. H.; Butler, J., *Advances in Free Radical Biology & Medicine* **1985**, 1, 91-131.
4. N. H. Attanayake, S. C. Abeyweera, A. C. Thenuwara, B. Anasori, Y.

Gogotsi, Y. Sun and D. R. Strongin, *Journal of Materials Chemistry A*, **2018**, 6, 16882-16889.

5. J. Liu, Y. Liu, D. Xu, Y. Zhu, W. Peng, Y. Li, F. Zhang and X. Fan, *Applied Catalysis B: Environmental*, **2019**, 241, 89-94.
6. L. Huang, L. Ai, M. Wang, J. Jiang and S. Wang, *International Journal of Hydrogen Energy*, **2019**, 44, 965-976.
7. L. Zhang, L. Wu, J. Li and J. Lei, *BMC Chemistry*, **2019**, 13, 88.
8. Z. Liu, X. Zhang, B. Wang, M. Xia, S. Gao, X. Liu, A. Zavabeti, J. Z. Ou, K. Kalantar-Zadeh and Y. Wang, *The Journal of Physical Chemistry C*, **2018**, 122, 12589-12597.
9. Z. Ye, J. Yang, B. Li, L. Shi, H. Ji, L. Song and H. Xu, *Small*, **2017**, 13, 1700111.
10. J. Ren, H. Zong, Y. Sun, S. Gong, Y. Feng, Z. Wang, L. Hu, K. Yu and Z. Zhu, *CrystEngComm*, **2020**, 22, 1395-1403.